A DFT Study of the Full Catalytic Cycle of the Suzuki−Miyaura Cross-Coupling on a Model System

Ataualpa A. C. Braga,[†] Gregori Ujaque,[‡] and Feliu Maseras*[,†,‡]

Institute of Chemical Research of Catalonia (ICIQ), 43007 Tarragona, Catalonia, Spain, and Unitat de Química Física, Edifici Cn, Universitat Autònoma de Barcelona, 08193 Bellaterra, Catalonia, Spain

Received May 2, 2006

A computational study with the Becke3LYP DFT functional is carried out on the cross-coupling reaction of vinyl bromide $H_2C{=}CHBr$ and vinylboronic acid $H_2C{=}CHB(OH)_2$ catalyzed by palladium diphosphine $[Pd(PH_3)_2]$ in the presence of an excess of base OH^-. The full catalytic cycle is computed, starting from the separated reactants and the catalyst and finishing with the cross-coupled product and the regeneration of the catalyst. The different stages in the cycle (oxidative addition, isomerization, transmetalation, reductive elimination) are characterized through calculation of the corresponding intermediates and transition states. Different alternative mechanisms are considered, depending on the number of phosphine ligands at palladium, and on the *cis* or *trans* isomery around the metal center. The results indicate the existence of a number of competitive pathways of reasonably low energy.

1. Introduction

The Suzuki−Miyaura cross-coupling reaction is one of the most widely used methods for the formation of carbon−carbon bonds. This reaction consists of the coupling between an organoboron compound and an organic halide (or triflate), mediated by a palladium catalyst in the presence of a base (eq 1).[1−3]

$$RB(OH)_2 + R'X \xrightarrow[\text{base}]{[Pd]} RR' + XB(OH)_2 \qquad (1)$$

Figure 1 presents the generally accepted textbook mechanism for the Suzuki−Miyaura cross-coupling. There are three main steps: (a) oxidative addition, (b) transmetalation, and (c) reductive elimination. Two of these main steps, oxidative addition and reductive elimination, are present also in a number of other processes in organometallic chemistry. Because of this, they have been repeatedly studied by experimental[4−6] and computational[7−11] chemistry and are currently quite well understood. It is generally accepted that both oxidative addition and reductive elimination need the involved ligands to be *cis* positioned, which together with the assumption of the trans-

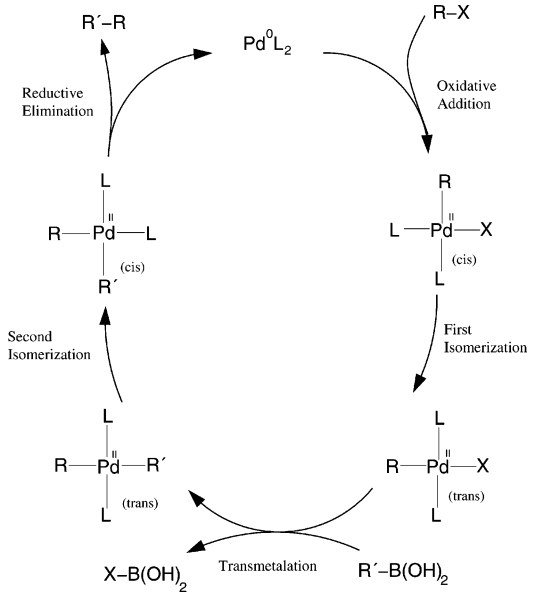

Figure 1. Generally accepted mechanism for the Suzuki−Miyaura cross-coupling.

metalation step taking place in the *trans* isomer requires the introduction of the two additional isomerization steps.[1,4]

The transmetalation process is specific to cross-coupling reactions, and because of this, fewer data are available. Experimental characterization is complicated because of the difficulty of isolating and characterizing the key intermediates,[12,13] but some progress has been made.[14−18] Computational studies with DFT methods on the transmetalation step of cross-

* To whom correspondence should be addressed. E-mail: fmaseras@iciq.es.
† ICIQ.
‡ Universitat Autònoma de Barcelona.

(1) Miyaura, N.; Suzuki, A. *Chem. Rev.* **1995**, *95*, 2457.
(2) Littke, A. F.; Fu, G. C. *Angew. Chem., Int. Ed.* **2002**, *41*, 4176.
(3) Espinet, P.; Echavarren, A. M. *Angew. Chem., Int. Ed.* **2004**, *43*, 4704.
(4) Casado, A. L.; Espinet, P. *Organometallics* **1998**, *17*, 954.
(5) Barrios-Landeros, F.; Hartwig, J. F. *J. Am. Chem. Soc.* **2005**, *127*, 6944.
(6) Gillie, A.; Stille, J. K. *J. Am. Chem. Soc.* **1980**, *102*, 4933.
(7) Sundermann, A.; Uzan, O.; Martin, J. M. L. *Chem. Eur. J.* **2001**, *7*, 1703.
(8) Goossen, L. J.; Koley, D.; Hermann, H.; Thiel, W. *Organometallics* **2005**, *24*, 2398.
(9) Ananikov, V. P.; Musaev, D. G.; Morokuma, K. *J. Am. Chem. Soc.* **2002**, *124*, 2839.
(10) Senn, H. M.; Ziegler, T. *Organometallics* **2004**, *23*, 2980.
(11) Zuidema, E.; van Leeuwen, P. W. N. M.; Bo, C. *Organometallics* **2005**, *24*, 3703.
(12) Aliprantis, A. O.; Canary, J. W. *J. Am. Chem. Soc.* **1994**, *116*, 6985.
(13) Nishihara, Y.; Onodera, H.; Osakada, K. *Chem. Commun.* **2004**, 192.
(14) Aramendia, M. A.; Lafont, F.; Moreno-Mañas, M.; Pleixats, R.; Roglans, A. *J. Org. Chem.* **1999**, *64*, 3592.
(15) Amatore, C.; Jutand, A. *Acc. Chem. Res.* **2000**, *33*, 314.
(16) Miyaura, N. *J. Organomet. Chem.* **2002**, *653*, 54.
(17) Stambuli, J. P.; Bühl, M.; Hartwig, J. F. *J. Am. Chem. Soc.* **2002**, *124*, 9346.
(18) Clarke, M. L.; Heydt, M. *Organometallics* **2005**, *24*, 6475.

10.1021/om060380i CCC: $33.50
Publication on Web 06/15/2006

coupling processes have started to appear in recent years concerning the reactions of Suzuki−Miyaura,[19−22] Stille,[23,24] and others.[25,26] In particular, we were able to demonstrate in a recent work[20] the importance of the presence of the base and that it acts by binding initially to the organoboronic acid rather than to the palladium species.

The fact that all the steps of the cross-coupling process are now more or less well understood does not fully explain the mechanistic details of the reaction. There are in particular two questions that require the study of the full cycle. The first of them is how many ligands are attached to palladium throughout the process. It is well known that the reaction runs often with catalyst precursors where two ligands, phosphines in the more conventional versions, are present. The assumption that the two phosphines stay throughout the whole reaction, implicit in fact in Figure 1, is thus reasonable. However, the use of bulky phosphines is known to increase performance in some cases, and it has been proposed that in these cases a monophosphine species can act as catalyst.[5,17,27−30] The second topic requiring the study of the full cycle concerns the *cis*/*trans* nature of intermediates and the need for isomerization steps. Oxidative addition of an organic halide to Pd^0L_2 produces a *cis* complex. This species has been seldom isolated,[4,31] and it is usually assumed that it isomerizes quickly to the *trans* form, which has often been characterized. One could however imagine a process where the transmetalation takes place directly on the *cis* isomer, and no isomerization is required.

Computational characterizations of the full cycle of the Suzuki−Miyaura cross-coupling processes have been recently published by the groups of Sakaki[19] and Thiel.[21,32] These studies have focused on rather specific substrates, the former on the coupling of iodobenzene with diboron, and the latter on the coupling of carboxylic anhydrides with arylboronic acids. Interestingly, Goossen and Thiel concluded that there are several interconnected catalytic pathways that may contribute to catalytic turnover.[21] In this work we present the computational characterization of the full Suzuki−Miyaura catalytic cycle for a system modeling the textbook form of this process, namely, the coupling between aryl bromides and arylboronic acids catalyzed by diphosphine palladium complexes.

Our computational model is defined by CH_2═CHBr, **1**, and CH_2═$CHB(OH)_2$, **2**, as reactants, $Pd(PH_3)_2$, **3**, as catalyst, and OH^- as base. The replacement of aryl by vinyl is straightforward; both of them have been experimentally shown to behave in a similar way, and we have computationally demonstrated that the transmetalation reaction is very similar for both substrates.[22] The use of PH_3 as phosphine is certainly a more critical approximation, but it is consistent with our intention to keep the model as general as possible. Furthermore, our previous work[20] showed that the steric effects of the phenyls in triphenylphosphine have little effect on the transmetalation profile. The goal of the current work is to critically evaluate the different mechanistic possibilities (one or two phosphines, *cis* or *trans* isomers) for the Suzuki−Miyaura cross-coupling on a general model system and see how the different reaction steps can be connected into a fully consistent mechanistic cycle.

2. Computational Methods

All calculations were performed at the DFT level, by means of the hybrid Becke3LYP[33−35] functional, with a hybrid Becke3 exchange functional and a Lee−Yang−Parr correlation functional[33,34] as implemented in Gaussian03.[36] Pd and Br atoms were described using an effective core potential (LANL2DZ) for the inner electrons[36,37] and its associated double-ζ basis set for the outer ones. In the case of Br atom, d-polarization functions were added (exponent 0.4280).[38] The 6-31G(d) basis set was used for the atoms H, B, C, O, and P.[39] Diffuse functions were added for B, C, O, P,[40] and Br[41] in the calculations involving anionic species, as well as in the bond dissociation energy calculations. Solvent effects were introduced in selected cases through PCM single-point calculations[42] on gas phase optimized geometries. The structures of the reactants, intermediates, transition states, and products were fully optimized without any symmetry restriction. Transition states were identified by having one imaginary frequency in the Hessian matrix.

3. The Problem of the Ligand Dissociation Energy

One of the goals of this work is to analyze whether the two phosphine ligands stay attached to the palladium center throughout the catalytic cycle. The formally simplest approach to the topic would be to compute the energy required for the dissociation of a palladium−phosphorus bond and to compare it with the barrier for alternative reaction pathways. Unfortunately, reliable calculation of bond dissociation energies in solution, albeit possible, is quite sensitive to the computational method. Bimolecular reactions, where one molecule breaks into two, have large entropic effects in the gas phase, and it is not clear to what extent these entropic effects are conserved in solution. We analyze in this section the bond dissociation energy of phosphine and bromide ligands from a number of palladium complexes.

The optimized geometries for the species considered in these dissociation reactions are included in Figures 2 and 3. Figure 2 presents the four tetracoordinate palladium complexes potentially

(19) Sumimoto, M.; Iwane, N.; Takahama, T.; Sakaki, S. *J. Am. Chem. Soc.* **2004**, *126*, 10457.
(20) Braga, A. A. C.; Morgon, N. H.; Ujaque, G.; Maseras, F. *J. Am. Chem. Soc.* **2005**, *127*, 9298.
(21) Goossen, L. J.; Koley, D.; Hermann, H.; Thiel, W. *Organometallics* **2006**, *25*, 54.
(22) Braga, A. A. C.; Morgon, N. H.; Ujaque, G.; Lledós, A.; Maseras, F. *J. Organomet. Chem.*, in press.
(23) Napolitano, E.; Farina, V.; Persico, M. *Organometallics* **2003**, *22*, 4030.
(24) Álvarez, R.; Faza, O. N.; López, C. S.; de Lera, A. R. *Org. Lett.* **2006**, *8*, 35.
(25) Kozuch, S.; Amatore, C.; Jutand, A.; Shaik, S. *Organometallics* **2005**, *24*, 2319.
(26) Garcia-Cuadrado, D.; Braga, A. A. C.; Maseras, F.; Echavarren, A. M. *J. Am. Chem. Soc.* **2006**, *128*, 1066.
(27) Walker, S. D.; Barder, T. E.; Martinelli, J. R.; Buchwald, S. L. *Angew. Chem., Int. Ed.* **2004**, *43*, 1871.
(28) Barder, T. E.; Walker, S. D.; Martinelli, J. R.; Buchwald, S. L. *J. Am. Chem. Soc.* **2005**, *127*, 4685.
(29) Christmann, U.; Vilar, R. *Angew. Chem., Int. Ed.* **2005**, *44*, 366.
(30) Chang, Y.-C.; Lee, J.-C.; Hong, F.-E. *Organometallics* **2005**, *24*, 5686.
(31) Urata, H.; Tanaka, M.; Fuchikami, T. *Chem. Lett.* **1987**, 751.
(32) Goossen, L. J.; Koley, D.; Hermann, H.; Thiel, W. *J. Am. Chem. Soc.* **2005**, *127*, 11102.
(33) Lee, C.; Parr, R. G.; Yang, W. *Phys. Rev. B* **1988**, *37*, 785.
(34) Becke, A. D. *J. Chem. Phys.* **1993**, *98*, 5648.
(35) Stephens, P. J.; Devlin, F. J.; Chabalowski, C. F.; Frisch, M. J. *J. Phys. Chem.* **1994**, *98*, 11623.
(36) Frisch, M. J.; et al. *Gaussian 03*, Revision C.02; Gaussian Inc.: Wallingford, CT, 2004.
(37) Wadt, W. R.; Hay, P. J. *J. Chem. Phys.* **1985**, *82*, 284.
(38) Höllwarth, A.; Böhme, M.; Dapprich, S.; Ehlers, A. W.; Gobbi, A.; Jonas, V.; Köhler, K. F.; Stegmann, R.; Veldkamp, A.; Frenking, G. *Chem. Phys. Lett.* **1993**, *208*, 237.
(39) Francl, M. M.; Pietro, W. J.; Hehre, W. J.; Binkley, J. S.; Gordon, M. S.; Defrees, D. J.; Pople, J. A. *J. Chem. Phys.* **1982**, *77*, 3654.
(40) Clark, T.; Chandrasekhar, J.; Spitznagel, G. W.; Schleyer, P. *J. Comput. Chem.* **1983**, *4*, 294.
(41) Check, C. E.; Faust, T. O.; Bailey, J. M.; Wright, B. J.; Gilbert, T. M.; Sunderlin, L. S. *J. Phys. Chem. A* **2001**, *105*, 8111.
(42) Miertus, S.; Scrocco, E.; Tomasi, J. *Chem. Phys.* **1981**, *55*, 117.

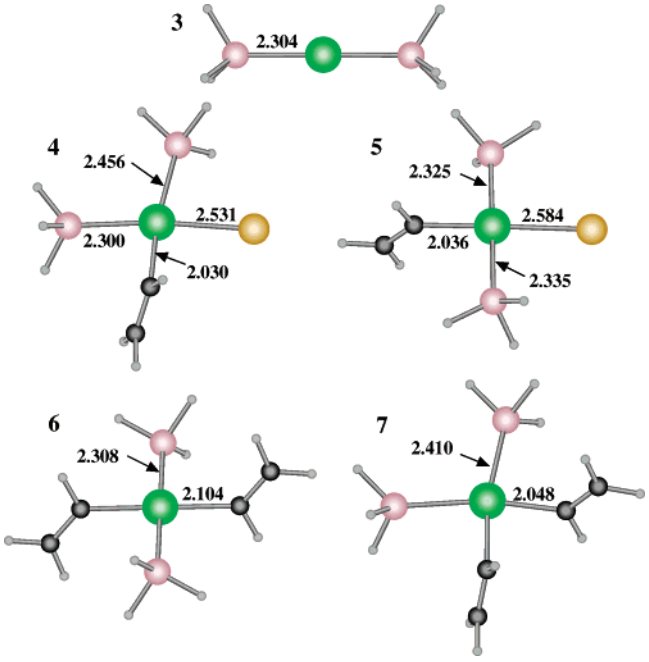

Figure 2. Becke3LYP-optimized geometries of tetracoordinate palladium complexes potentially involved in the catalytic cycle, together with the diphosphine parent complex.

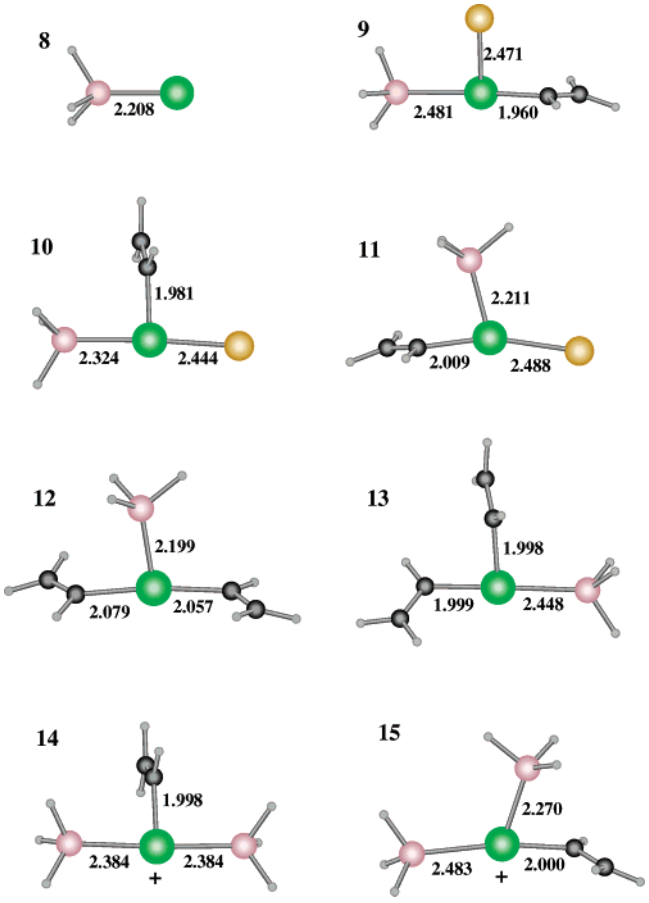

Figure 3. Becke3LYP-optimized geometries of tricoordinate palladium complexes potentially involved in the catalytic cycle together with the monophosphine complex.

present in the catalytic cycle, together with the starting diphosphine complex **3**. If no free phosphine is released, the oxidative addition produces species of general formula $Pd(PH_3)_2(Br)(HC{=}CH_2)$, which can be either *cis* (**4**) or *trans* (**5**). Similarly, after the transmetalation, where bromide is replaced by a second vinyl ligand, the *trans* (**6**) and *cis* (**7**) isomers of $Pd(PH_3)_2(HC{=}CH_2)_2$ are possible. Figure 3 collects the tricoordinate palladium complexes. If only one phosphine ligand is present, oxidative addition results in T-shaped $Pd(PH_3)(Br)(HC{=}CH_2)$ species, and three isomers are possible, depending on whether the apical site is occupied by bromide (**9**), vinyl (**10**), or phosphine (**11**). After transmetalation, the $Pd(PH_3)(HC{=}CH_2)_2$ complex has two possible isomers, as only phosphine (**12**) or vinyl (**13**) can be in the apical position. Figure 3 includes also two isomers of $Pd(PH_3)_2(HC{=}CH_2)^+$ (**14**, **15**), which can result from bromide dissociation of the oxidative addition products, and the monophosphine starting complex **8**.

Table 1. Computed Values (kcal/mol) for Magnitudes Related to the Ligand Dissociation Process

entry	reaction	ΔE	ΔG	ΔE_{solv}	ΔG_{solv}
1	**4** → **10** + PH_3	16.1	2.3	12.3	−1.5
2	**4** → **9** + PH_3	25.4	10.0	27.5	12.1
3	**5** → **11** + PH_3	24.8	11.3	15.1	1.6
4	**4** → **15** + Br^-	121.0	111.3	19.0	9.3
5	**5** → **14** + Br^-	121.1	111.8	17.6	8.4
6	**3** → **8** + PH_3	26.8	17.2	19.1	9.4
7	**6** → **12** + PH_3	25.6	12.2	19.9	6.5
8	**7** → **13** + PH_3	16.1	1.6	15.1	0.6

Table 1 presents the computed energy values for the ligand dissociation reactions involving a variety of the species shown in Figures 2 and 3. Four different values are presented for each reaction. The first column, ΔE, represents the potential energy. It comes directly from the SCF part of the quantum chemical calculation. It is the most straightforward value from the calculation, but it is not directly connected to any experimental parameter. The values corresponding to the phosphine dissociation processes (lines 1, 2, 3, 6, 7, 8) are between 16.1 and 26.8 kcal/mol. The smallest value, 16.1 kcal/mol, is that of the phosphine *trans* to vinyl, showing the large *trans* influence of this ligand. The four other phosphine dissociation values in this column are within a span of 2 kcal/mol (from 24.8 to 26.8). The values associated with bromide dissociation processes are much higher (ca. 121 kcal/mol), because this reaction involves charge separation, and this is completely disfavored in a vacuum. The second column contains the Gibbs free energy values in the gas phase, ΔG. The Gibbs free energy is obtained by adding zero-point, thermal, and entropy corrections to the potential energy. In the particular set of reactions involving PH_3 dissociation, all ΔG values are smaller than the corresponding ΔE, the difference being between 9.3 and 15.4 kcal/mol. The reduction is essentially associated with the entropy factor, which strongly favors the formation of two fragments from a single molecule. The trends from the ΔE column are practically unchanged in the second column.

The last two columns correspond to the introduction of solvation. The solvent considered is water, with a high dielectric constant. The idea is estimating the maximum possible effect of the solvent in this process. The third column, ΔE_{solv}, results from adding the contribution of the free energy of solvation to the potential energy. As expected, the solvent effect on the reactions involving bromide dissociation are huge, over 100 kcal/mol with respect to the ΔE values. The solvent stabilizes much better the separated charges. For the phosphine dissociation reaction, solvation effects are smaller. This ΔE_{solv} value includes the free energy effects of the solvent, but not those of the solute. The solute contribution ΔG_{solv} can be obtained from adding the gas free energy corrections of the solute to ΔE_{solv}, as indicated in eq 2.

$$\Delta G_{solv} = \Delta E_{solv} + (\Delta G - \Delta E) \quad (2)$$

The fourth column collects the values for ΔG_{solv} of the different dissociation processes considered. ΔG_{solv} should be, in principle, the most accurate value, because it would represent the Gibbs free energy in solution. It is remarkable however that the dissociation energy values come out very small in this last column, with that in the first row being in fact negative (−1.5 kcal/mol). This would mean that the *cis*-$Pd(PH_3)_2(Br)(HC{=}CH_2)$ complex would spontaneously lose the phosphine *trans* to vinyl.

This method for the calculation of the free energy associated with a bimolecular reaction in solution is not exact. The large free energy correction in the gas phase is strongly associated with the increase in entropy. Entropy grows mostly in its translation and rotation components. When the initial molecule splits in two, the fragments can move independently, which largely benefits the entropy of the whole system. The problem is that this is not necessarily a good approach for the situation in solution, where the translation and rotation of the separated fragments will be constrained by the presence of solvent molecules. In view of this problem, Sakaki and co-workers[19,43,44] proposed the use of a modified free energy correction where only the vibration contributions to entropy are considered, and those coming from translation and rotation are neglected. This is not exact either, because the solvent constrains the movement of the separate fragments, but does not suppress it. The use of this approach results in values that are much closer to those of the potential energy. For instance, for the reaction in the first row of Table 1, the modified formula would result in values of 15.6 kcal/mol for ΔG^{mod} (gas phase) and 11.8 kcal/mol for ΔG^{mod}_{solv} (solution). These values are only 0.5 kcal/mol lower than the corresponding ΔE values, but 12.3 kcal/mol above those of ΔG. The correct value for the Gibbs free energy of dissociation in solution lies between those of ΔG_{solv} and ΔG^{mod}_{solv}, probably closer to the latter, but no simple method is available, within the simple continuum PCM approach, to assign a precise value to it.

Regardless of the difficulty in the choice of the correct magnitude, a significant result can be extracted from Table 1 concerning the process under study. In complexes **4** and **5**, where both phosphine and bromine are present, phosphine dissociation is preferred. If we compare rows 1 and 4, for the *cis* complex **4**, the difference in ΔE_{solv} is 6.7 kcal/mol in favor of phosphine dissociation, and this is the magnitude where the difference is smallest. The comparison of rows 3 and 5, corresponding to the *trans* complex **5**, shows a difference in ΔE_{solv} of 2.5 kcal/mol. The fact that phosphine dissociation is easier in all energy scales than bromide dissociation, even in a highly polar solvent as water, suggests strongly that the so-called cationic mechanism, which is operative in Heck reactions where triflate acts as leaving group,[45] is quite unlikely in the Suzuki−Miyaura cross-coupling with organic bromide molecules.

Table 1 is easy to interpret when all magnitudes follow the same trend, but it is difficult to choose one particular magnitude for use in the catalytic cycle. A more detailed study, beyond the scope of this work, should be carried out to obtain an estimation of dissociation energy of comparable quality to that of other reaction steps. Furthermore, such calculations would have to incorporate real substituents, because the specific values for experimental phosphines will be probably not well represented by PH_3 or PMe_3 models. Because of this, we have decided to keep the energetics of these dissociation processes outside our computed profiles. We have defined two independent mechanisms: one with a diphosphine system, which we label as associative, and the other one with a monophosphine system, labeled as dissociative. The full catalytic cycle is computed for each of the cycles in the next two sections, and the results are globally discussed afterward.

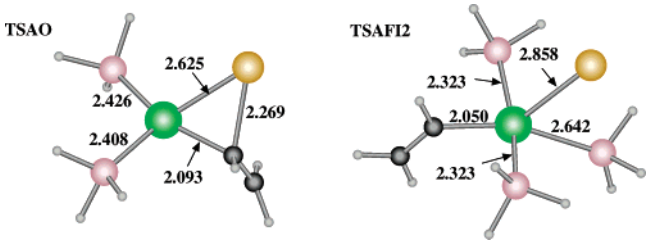

Figure 4. Becke3LYP-optimized geometries for the transition states corresponding to the oxidative addition (TSAO) and first isomerization (TSAFI2) steps of the associative mechanism.

4. Diphosphine System (Associative Mechanism)

We first discuss the case where palladium retains the two phosphine ligands throughout the main steps of the catalytic cycle. This associative mechanism is likely operative for chelating phosphines and seems at least a reasonable alternative for monophosphine ligands with small to moderate steric bulk. The different steps of the mechanism are analyzed in what follows.

4.1. Oxidative Addition. In the oxidative addition step, the bond between the organic group and the halide atom breaks, and two new bonds are formed with palladium, which in this way increases its oxidation state from 0 to +2. This is shown in eq 3.

$$L_nPd + R - X \rightarrow L_nPd(R)(X) \quad (3)$$

The oxidative addition of aryl halides to linear Pd^0L_2 complexes has been shown by previous experimental[4,46] and computational[8,47] studies to be a concerted process leading to the formation of a *cis* square planar complex. Our calculations confirm this result. The complex *cis*-$CH_2{=}CHPdBr(PH_3)_2$, **4** (Figure 2), is the product obtained from the oxidative addition of $CH_2{=}CHBr$, **1**, to the palladium catalyst $Pd(PH_3)_2$, **3**.

The transition state for this process, shown in Figure 4, is labeled **TSAO**. The criteria for the labeling, which will be followed for all intermediate and transition states throughout the article, are **TS** for **t**ransition **s**tate, **A** for **a**ssociative mechanism, and **O** for **o**xidative addition. In transition state **TSAO** the computed P−P−Pd−Br dihedral angle is 139.7°. The planes P−Pd−P and Br−Pd−C are thus not aligned, in agreement with the results in previous computational works.[7,48] Before reaching **TSAO**, the initial approach between the reactants produces intermediate **IAO**, where the alkene is coordinated η^2 to the metal center, with Pd−C distances of 2.161 and 2.197 Å. **IAO** has a potential energy 11.1 kcal/mol below that of the separate reactants. The overall thermodynamics of this step are exothermic: **4** is 12.7 kcal/mol more stable than

(43) Tamura, H.; Yamasaki, H.; Sato, H.; Sakaki, S. *J. Am. Chem. Soc.* **2003**, *125*, 16114.
(44) Sakaki, S.; Takayama, T.; Sumimoto, M.; Sugimoto, M. *J. Am. Chem. Soc.* **2004**, *126*, 3332.
(45) Balcells, D.; Maseras, F.; Keay, B. A.; Ziegler, T. *Organometallics* **2004**, *23*, 2784.
(46) Jutand, A.; Négri, S. *Organometallics* **2003**, *22*, 4229.
(47) Albert, K.; Gisdakis, P.; Rösch, N. *Organometallics* **1998**, *17*, 1608.
(48) Sakaki, S.; Mizoe, N.; Musashi, Y.; Biswas, B.; Sugimoto, M. *J. Phys. Chem. A* **1998**, *102*, 8027.

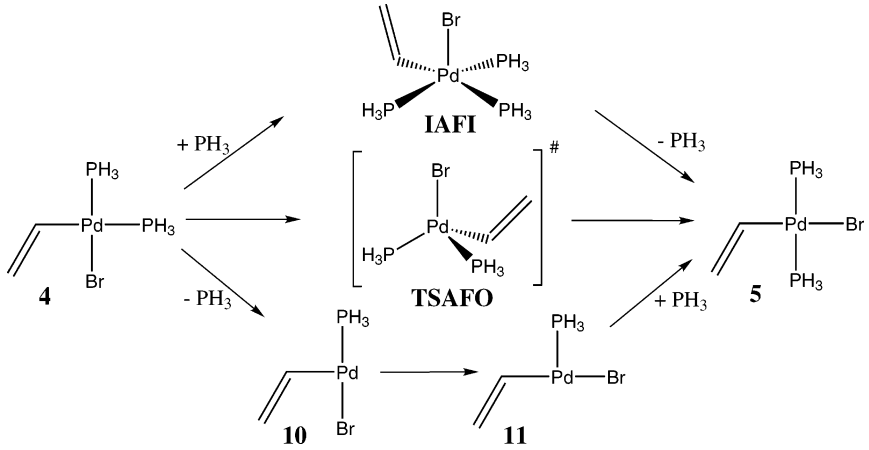

Figure 5. The three possible alternatives for the isomerization from the *cis* to the *trans* form of CH_2═$CHPdBr(PH_3)_2$.

the reactants **1** plus **3**. **TSAO** is 9.7 kcal/mol above the reactants and 20.8 kcal/mol above intermediate **IAO**. The relatively high value of the barrier is consistent with the fact that oxidative addition has been often proposed as the rate-determining step of the catalytic cycle.[49,50]

4.2. First Isomerization. Despite the fact that the square planar *cis* isomer is generally accepted as the product of the oxidative addition, it has been seldom isolated.[4,31] The transmetalation process is in fact usually assumed to take place from the *trans* square planar complex **5**. We will consider in the next section the two possible transmetalation mechanisms, starting from the *cis* and *trans* isomers. We discuss here the possible interconversion mechanism between these two isomers, which must take place before the transmetalation. The process is shown in eq 4. Intermediates and transition states in this mechanism will carry the label **F** (for first isomerization).

$$cis\text{-}L_nPd(R)(X) \rightarrow trans\text{-}L_nPd(R)(X) \qquad (4)$$

The interconversion is practically thermoneutral, with the *trans* isomer 4.6 kcal/mol below the *cis* species, but the mechanism is not evident. In principle, the associative first isomerization step has the three possible variations summarized in Figure 5: (i) direct f**o**ur-coordinate rearrangement (label **O**) via a tetrahedral transition state **TSAFO**, (ii) **t**hree-coordinate rearrangement (label **T**), with initial loss of a phosphine ligand, passing through complexes **10** and **11**, and (iii) f**i**ve-coordinate rearrangement (label **I**), through initial incorporation of an external ligand to the palladium coordination sphere and formation of intermediate **IAFI**.

The formally simplest mechanism is of course the four-coordinate one, with no need for change in the coordination number. We succeeded in optimizing the transition state for this process **TSAFO**, which is in fact quasi-tetrahedral. The energy barrier is however quite high, 20.3 kcal/mol, similar in fact to the value reported by Thiel and co-workers[8] for the analogous process involving the $PhPdI(PMe_3)_2$ complex. This relatively high barrier is explained by the low stability of tetrahedral d^8 arrangements associated with the population of antibonding orbitals.

Experimental work by Espinet and co-workers[4,51] led to the suggestion that the isomerization process is carried out in two stages, the first of them being a phosphine dissociation, which leads to a three-coordinate complex. We thus analyzed the isomerization process involving the T-shaped monophosphine complexes **10** and **11** (Figure 3). **10** can be obtained from dissociating the phosphine *trans* to vinyl in the *cis* square planar species **4**, and **11** can produce the *trans* square planar species **5** by simple binding of a phosphine group to the vacant site. As happened for the four-coordinate mechanism, in this three-coordinate mechanism, the conversion from **10** to **11** is also almost thermoneutral; in this case the *cis* isomer **10** is more stable by 4.2 kcal/mol. However, the energy barrier is significantly lower for the three-coordinate mechanism. The Y-shaped transition state **TSAFT** is only 4.5 kcal/mol above **10**. This three-coordinate mechanism appears thus as quite favorable, always after the phosphine dissociation from the initial catalyst can be achieved.

The third mechanism that can be proposed to explain the isomerization process starts with the formation of a five-coordinate species with inclusion of an external ligand. This external ligand may in principle be a phosphine, a solvent molecule, a free anion, or a substrate molecule. For this work, we used phosphine as a representative example. A smooth reaction profile could be optimized, going through a five-coordinate intermediate **IAFI**, which has a square pyramidal geometry with the bromide ligand in the axial position. This intermediate has an energy 2.3 kcal/mol above the *cis* complex **4** plus phosphine. **IAFI** is connected to **4** by transition state **TSAFI1**, with a relative energy of 2.7 kcal/mol, and to **5** through **TSAFI2**, shown in Figure 4, with a relative energy of 5.5 kcal/mol. This is a low barrier, indicative of a feasible step, a result that has to be again taken with caution because the process involves a change in the number of ligands.

The calculations presented in this subsection indicate thus that the direct *cis*/*trans* four-coordinate rearrangement has a quite high barrier, but that there are alternative mechanisms possible, involving either phosphine dissociation or association of an external ligand. It is difficult to compute an accurate barrier for these alternative paths because of the considerations mentioned in the previous section, but it seems quite safe to assume that these barriers will be low in most systems. Therefore, this isomerization step should not be a critical obstacle for the overall cross-coupling process.

4.3. Transmetalation. The transmetalation process is the stage where the migration of the organic group from the organoboronic acid to the palladium complex takes place, as shown in eq 5.

(49) Smith, G. B.; Dezeny, G. C.; Hughes, D. L.; King, A. O.; Verhoeven, T. R. *J. Org. Chem.* **1994**, *59*, 8151.
(50) Matos, K.; Soderquist, J. A. *J. Org. Chem.* **1998**, *63*, 461.
(51) Casado, A. L.; Casares, J. A.; Espinet, P. *Inorg. Chem.* **1998**, *37*, 4154.

$$L_n(R)Pd - X + R' - B(OH)_2 \rightarrow L_n(R)Pd - R' + X - B(OH)_2 \quad (5)$$

In contrast with other parts of the catalytic cycle, this step is specific to cross-coupling reactions. Understanding of its mechanistic subtleties has been significantly helped by recent computational studies.[19−22,24,32] In particular, in a previous work[20] we could explain the role of the base that has to be necessarily added for the reaction to take place. It was found that the base attacks first the boronic acid, producing an anionic organoboronate intermediate, which can afterward attack the palladium complex and produce the transmetalation. In this previous study, we assumed that the palladium retained two phosphine ligands through the transmetalation and that they were in a *trans* arrangement. This *trans* arrangement is in the textbook mechanism, but we have shown above that the oxidative addition produces a *cis* intermediate, and we will consider the *cis*/*trans* alternative in what follows.

The first transmetalation path discussed will be the associative *trans* (ATT) mechanism. It had been already fully characterized in our previous work,[20] and we are providing it here only for completeness. The energy profile for this transmetalation is summarized in Figure 6. The process takes place in three stages. First, the organoboronate species replaces the bromide ligand, and the initial long-distance complex **IATT1** (−16.2 kcal/mol) evolves to the intermediate oxo-palladium species **IATT2** (−12.2 kcal/mol). In the second stage, the alkene replaces the hydroxyl ligand in the coordination sphere in the metal. Intermediate **IATT3** is formed, containing an η^2 coordination of the alkene, with an energy of −5.8 kcal/mol. Finally, in the last stage the divinyl complex *trans*-Pd−(CH═CH_2)$_2$(PH_3)$_2$ (**6**) is produced. The energy barrier to reach the transition state of this last step (**TSATT3**), which has the highest energy in the profile, was calculated to be only 4.2 kcal/mol above the separated reactants. The overall process is quite smooth, being exothermic by −21.0 kcal/mol. The difference between the energies of the highest energy transition state (**TSATT3**) and the lowest energy intermediate (**IATT1**) is 20.4 kcal/mol.

The alternative associative transmetalation pathway ATC connects the two *cis* species directly. Figure 7 presents the computed energy profile. The profile is qualitatively similar to that of path ATT. After the initial approach between species **4** and **16** to produce the long-distance intermediate **IATC1**, 26.1 kcal/mol below the separated reactants, the transmetalation takes place in three steps. The first step corresponds to the displacement of Br^- by one of the OH^- groups of **16**. In the corresponding transition state, **TSATC1**, shown in Figure 8, the distances of the breaking Pd−Br and forming Pd−O bonds were computed as 2.774 and 2.319 Å, respectively. In the subsequent intermediate (**IATC2**) there is a strong Pd−O bond (2.147 Å), and the bromide leaves the palladium coordination sphere (Pd−Br is 5.142 Å). The second step corresponds to the formation of an η^2 alkene complex **IATC3**. The vinylboronate ligand rearranges itself in this step, the Pd−O bond is broken, and two Pd−C bonds are formed in transition state **TSATC2**. The third and last step corresponds to the formation of the η^1 vinyl complex *cis*-(CH_2═CH)$_2$Pd(PH_3)$_2$, **7**, and the release of the boronic acid $B(OH)_3$ (**17**). In the corresponding transition state (**TSATC3**), shown in Figure 8, the distances of the forming Pd−C bond and the breaking C−B bond are 2.208 and 1.926 Å, respectively.

Similarly to what happened for the *trans* alternative, the energy profile for the *cis* associative transmetalation is smooth (Figure 7). The highest energy point, corresponding to **TSATC3**, the transition state for the last step, is below the separated reactants by 9.2 kcal/mol. The overall process is exothermic by 36.7 kcal/mol, with the products having the lowest energy. The difference between the energies of the highest energy transition state **TSATC3** and the lowest energy intermediate **IATC1** (the initial long-distance complex) is only 16.9 kcal/mol.

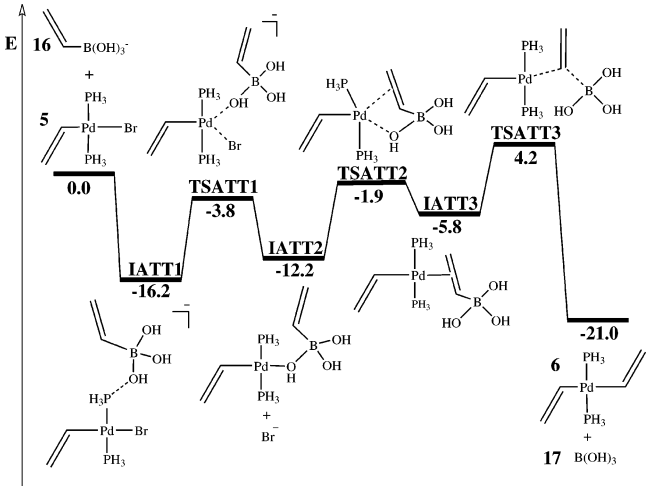

Figure 6. Energy profile for the *trans* alternative of the transmetalation step in the associative mechanism.

Most previous computational work on transmetalation had concentrated on *trans* arrangements,[19,20] with the notable exception of the recent work by Goossen, Thiel, and co-workers using the *cis*-CH_3C(═O)Pd(OAc)(PMe_3)$_2$ complex as a starting point.[21] In that work, smooth energy changes were also found, although the profile required an additional dissociation step. We think that the fundamental trends are the same as in the present study, and the minor qualitative discrepancies can be attributed to differences in the nature of the organic groups and the computational modeling of the phosphine ligands.

4.4. Second Isomerization. After the transmetalation, the reductive elimination must take place to release CH_2═CH−CH═CH_2, **18**, and regenerate the catalyst **3**. Reductive elimination requires the Pd complex to be in the *cis* configuration. Thus, in the cases where the transmetalation process has produced complexes in *trans* an additional *trans*-to-*cis* isomerization step is necessary. This is analogous to what happened after the oxidative addition, and we have labeled this step as **s**econd isomerization (label **S**). The process is shown in eq 6.

$$trans\text{-}L_nPd(R)(R') \rightarrow cis\text{-}L_nPd(R)(R') \quad (6)$$

There are a lot of analogies between the two isomerization steps, since the only difference between the two sets of complexes is one of the ligands, which is bromide in the first isomerization (complexes **4**, **5**) and vinyl in the second one (complexes **6**, **7**). The reaction is almost thermoneutral (3.7 kcal/mol in favor of **7**), and the three mechanisms reported above for the first isomerization are again available here.

A quasi-tetrahedral transition state, **TSASO**, was computed for the direct four-coordinate isomerization. In **TSASO** one of the phosphine ligands is close to dissociation, with a distance between P and Pd as long as 3.957 Å. The energy barrier to reach **TSASO** from **6** is high, up to 33.9 kcal/mol.

The alternative three-coordinate mechanism, with initial loss of a phosphine, appears quite feasible. The connection between the three-coordinate T-shaped complexes **12** and **13** goes through the Y-shaped transition state **TSAST**, shown in Figure

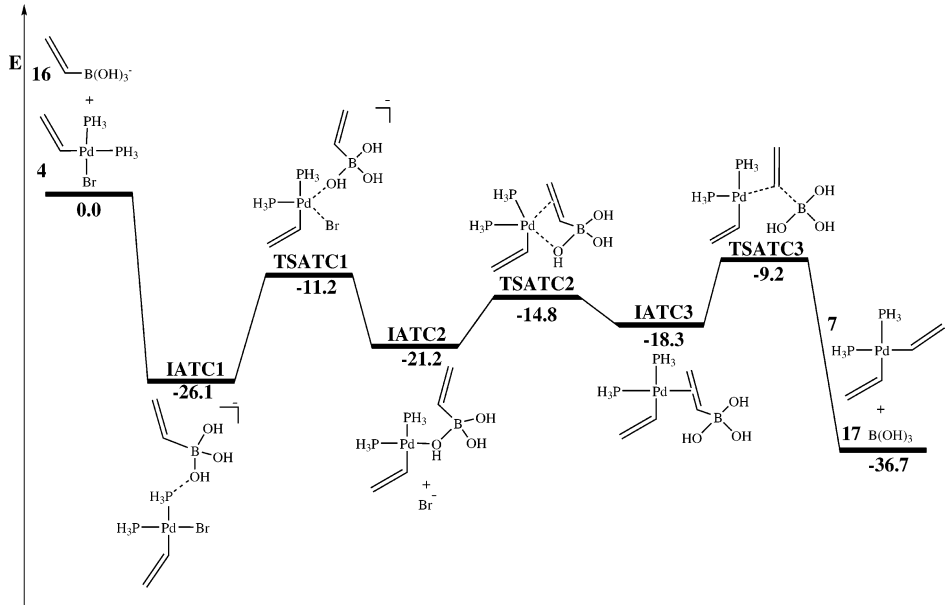

Figure 7. Energy profile for the *cis* alternative of the transmetalation step in the associative mechanism.

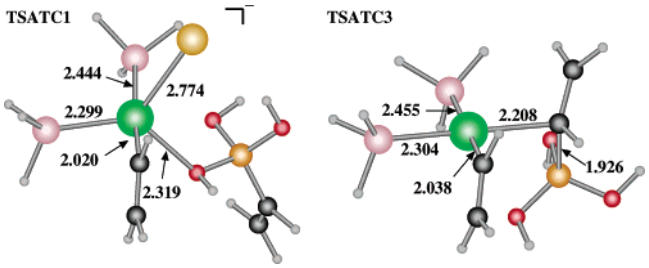

Figure 8. Becke3LYP-optimized geometries of selected transition states for the *cis* alternative of the transmetalation step in the associative mechanism.

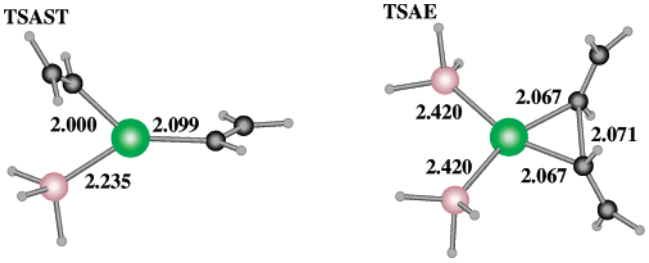

Figure 9. Becke3LYP-optimized geometries of selected transition states corresponding to the second isomerization (TSAST) and reductive elimination (TSAE) steps of the associative mechanism.

9. The angles P−Pd−C were computed as 173° in **12**, 85.2° in **15**, and 138.2° in the transition state, respectively. The reaction is moderately exothermic (13.5 kcal/mol), and the energy barrier is quite low (9.6 kcal/mol). The feasibility for this three-coordinate mechanism is again in agreement with previous experimental evidence.[51] Of course, the requirement for the phosphine dissociation is always present, with the difficulty to estimate accurately its energy.

In contrast with what happened for the first isomerization, the five-coordinate isomerization path has a high energy for the second isomerization. As happened for the bromide vinyl complex, the approach of an external phosphine to the metal originates a reaction path connecting the *trans* and *cis* isomers, but the similarities between both complexes stop there. In this second isomerization there are no intermediates, only one transition state, **TSASI**, and its energy is 32.3 kcal/mol above **6** plus phosphine. The reason for this high energy seems to be that the apical position in the square pyramidal **TSASI** is occupied by a vinyl group, which is strongly destabilizing in this partially antibonding site.

This second isomerization step, from the *trans* to *cis* isomers of the square planar divinyl complexes, seems to have less options than the initial isomerization and has to take place necessarily through loss of one of the phosphine ligands. Once this is accomplished, the barrier is nevertheless quite low.

4.5. Reductive Elimination. In the reductive elimination step, a bond between the two organic groups attached to the metal is made, and two previously existing bonds with palladium are broken, which in this way decreases its oxidation state from +2 to 0. This is shown in eq 7.

$$L_nPd(R)(R') \rightarrow L_nPd + R - R' \qquad (7)$$

In this associative mechanism, the reductive **e**limination process (**E**) has to start from the *cis* complex **7**. It proceeds through transition state **TSAE** (Figure 9) to intermediate **IAE**. The distance C−C between the vinyl groups evolves from 2.699 Å in **7** to 2.071 Å in transition state **TSAE**. In the resulting intermediate, **IAE**, this distance becomes 1.465 Å. The immediate result of reductive elimination is species **IAE**, which is a π complex. The presence of this kind of intermediate after reductive elimination had already been reported.[9,52] In this η^2 complex our computed Pd−C distances are 2.262 and 2.209 Å. The last step in the catalytic cycle is separation of the product (**18**) from the catalyst **3**, which is then ready to reinitiate the cycle. This last step has a moderate energy cost in terms of potential energy of 9.7 kcal/mol, which would be even smaller in terms of free energy because of the entropic factor involved in a bimolecular process.

The reductive elimination stage presents a small barrier of 4.8 kcal/mol, which is the relative energy of **TSAE** with respect to **7**. The overall process is furthermore strongly exothermic, with the starting palladium divinyl species **7** being 45.9 kcal/mol above the η^2 complex **IAE** and 36.2 kcal/mol above product plus catalyst.

(52) Albéniz, A. C.; Espinet, P.; Pérez-Mateo, A.; Nova, A.; Ujaque, G. *Organometallics* **2006**, *25*, 1293.

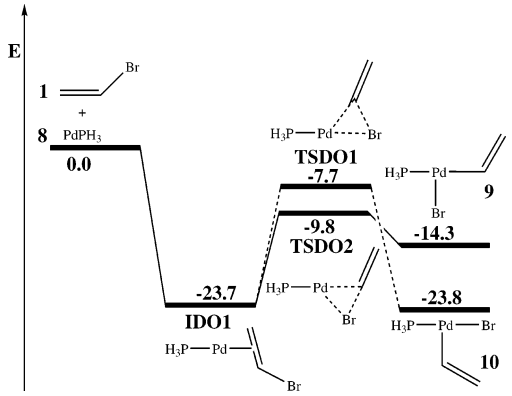

Figure 10. Energy profile for the oxidative addition step in the dissociative mechanism.

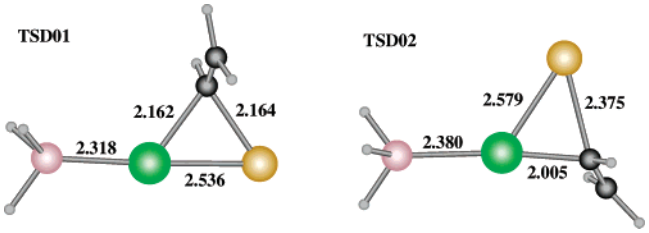

Figure 11. Becke3LYP-optimized geometries for the transition states corresponding to the oxidative addition step in the dissociative mechanism.

5. Monophosphine System (Dissociative Mechanism)

We turn now our attention to the dissociative mechanism, where a phosphine is lost before the catalytic cycle starts, and all the reactions take place with a monophosphine palladium species. This dissociative mechanism is likely to operate for bulky phosphines and is a possible alternative for phosphines with smaller steric bulk. The steps are similar to those for the associative mechanisms and are discussed in detail below.

5.1. Oxidative Addition. The oxidative addition of R−Br to the monophosphine LPd system produces a three-coordinate LPd(R)(Br) species. This d^8 complex has a T shape, and two different isomers are directly accessible from the separate reactants. As was the case for the associative mechanism, the two ligands being oxidatively added, vinyl and bromide, end up in a *cis* arrangement, but this does not fully define the structure of the complex. The phosphine ligand can finish in a position *trans* to vinyl (complex **9**) or *trans* to bromide (complex **10**).

Figure 10 presents the energy profiles for the two possible oxidative addition processes. Both of them start with the formation of a common intermediate, which is the η^2 alkene complex **IDO1**, with Pd−C bond distances of 2.223 and 2.166 Å. This is a quite stable species, 23.7 kcal/mol below the separated reactants. It is analogous in structure to the intermediate **IAO** reported above for the associative mechanism. The two paths differ from **IDO1**. One oxidative addition goes to complex **10**, with *trans* phosphine and bromide through transition state **TSDO1**, while the other goes to complex **9**, where phosphine is *trans* to vinyl, through transition state **TSDO2**. Both **TSDO1** and **TSDO2**, shown in Figure 11, have geometrical agreements indicative of cleavage of the C−Br bond. The C−Br distance, which is 1.941 Å in intermediate **IDO1**, increases to 2.164 Å in **TSDO1** and to 2.375 Å in **TSDO2**.

The energetics of the two oxidative addition processes are similar, but not identical. Complex **10**, with the phosphine and bromide ligands *trans*, is the most stable species, 0.1 kcal/mol below the η^2 species **IDO1** and 23.8 kcal/mol below the separated reactants. Transition state **TSDO1**, connecting **IDO1** and **10**, is 16.0 kcal/mol above **IDO1**. The second possible oxidative addition process goes to the *trans* phosphine vinyl species **9** through transition state **TSDO2**. The product is less stable (14.3 kcal/mol below reactants), but the energy barrier is lower (13.9 kcal/mol above **IDO1**).

The comparison of the oxidative addition between the monophosphine and the diphosphine systems shows that the reaction is thermodynamically and kinetically more favorable for the monophosphine systems. This is logical because the less saturated system increases more easily its coordination number by 2. It is furthermore consistent with the fact that systems with bulky phosphines, more likely to lose one ligand, are more active toward activation of difficult substrates such as aryl chlorides.[5,28]

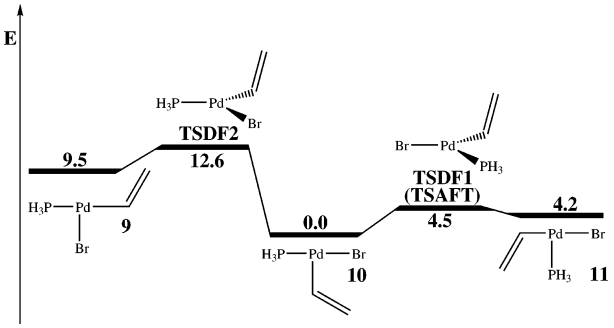

Figure 12. Energy profile for the first isomerization step in the dissociative mechanism.

5.2. First Isomerization. The transmetalation does not have to take place necessarily in the same ligand arrangement resulting from the oxidative addition, and an additional isomerization step is possible. For the monophosphine system, there are three possible T-shaped isomers LPd(R)(Br), **9**, **10**, and **11**, shown in Figure 3. Two of them, **9** and **10**, can be directly obtained from the oxidative addition step, as described above, while the other one, **11**, has a *trans* arrangement of bromide and vinyl. The most stable of the three species is **10** followed by **11**, 4.2 kcal/mol above, and the least stable is **9**, 9.5 kcal/mol above **10**.

We could find the transition states for two of the three possible interconversion processes, and the resulting energy profile is shown in Figure 12. The conversion between **10** and **11** had been in fact already treated above within the discussion on the three-coordinate variety of the first isomerization in the associative mechanism. The transition state for this step, which had been labeled as **TSAFT**, had a Y-shape and an energy of 4.5 kcal/mol above **10**. The conversion between **10** and **9** takes place through transition state **TSDF2**. **TSDF2** has the expected Y-shape. The Br−Pd−C bond angle maintains a value close to 90° (83.0°), while the phosphine ligand is in the apical position of the Y, with P−Pd−C and P−Pd−Br bond angles of 143.5° and 133.3°, respectively. The energy barrier is low, 12.6 kcal/mol above **10**, but only 3.1 kcal/mol above **9**. It is worth noticing that this result, coupled with those of the previous section, indicates that **10** is more easily accessible from the separated reactants going through complex **9** (transition states **TSDO2**, −9.8 kcal/mol, and **TSDF2**, −11.2 kcal/mol) than through one single step (transition state **TSDO1**, −7.7 kcal/mol).

Despite our efforts, we could not locate a direct transition state connecting the two higher energy isomers **9** and **11**. All our calculations converged to either one of the two previously reported transition states or the separated reactants. The absence

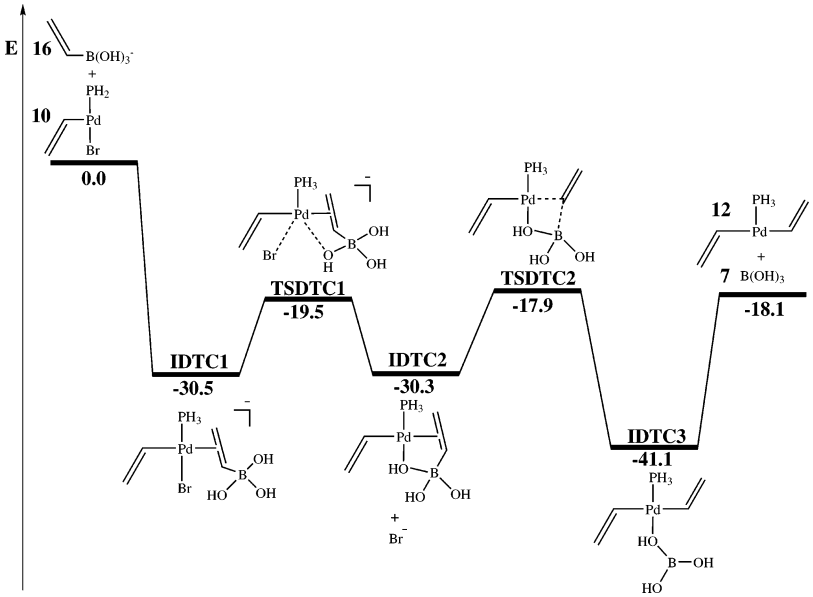

Figure 13. Energy profile for the *cis* alternative of the transmetalation step in the dissociative mechanism.

of this direct transition state has nevertheless little effect on the overall chemistry of the system, because the conversion can take place easily through isomer **10**.

5.3. Transmetalation. The next step in the Suzuki−Miyaura cross-coupling is the transmetalation, where the organic group originally attached to the boron atom replaces the bromide in the palladium coordination sphere. As happened in the case of the diphosphine systems, for the monophosphine systems, several isomers are possible for both the start and the end of transmetalation, and this results in the existence of different parallel paths. Of the three possible isomers of the T-shaped LPd(R)(Br) complex, only two of them are valid starting points for the transmetalation. Complex **9**, with bromide *trans* to the vacant site, cannot directly undergo the transmetalation. This is because the approaching organoboronate will occupy the vacant site (*trans* to bromide), and it must be *cis* to bromide for the exchange to take place.

The path starting from the three-coordinate complex **10** and CH_2═CH−$B(OH)_3^-$, **16**, has been labeled as dissociative transmetalation *cis* (DTC). Its profile is shown in Figure 13. The reaction starts with the formation of the olefin π complex **IDTC1**. It is quite stable, 30.5 kcal/mol below **10** plus **16**, because it corresponds to a strong interaction between the vacant site in the Pd center and the π orbital of the double bond in the vinyl substituent of the boronate anion. The bond distances of the Pd to the incoming carbons are 2.580 and 2.444 Å, respectively. The double bond is approximately coplanar with palladium, phosphorus, and bromine.

From this initial intermediate **IDTC1**, the reaction proceeds in two stages. In the first step, one of the hydroxyl groups of the boronate replaces the bromide from the palladium coordination sphere, and intermediate **IDTC2** is obtained via transition state **TSDTC1** (Figure 14). The process can be clearly followed by the evolution of the bond distances. The Pd−O distance changes from 3.519 Å in **IDTC1**, to 2.387 Å in **TSDTC1**, to 2.151 Å in **IDTC2**. The Pd−Br distance follows the opposite evolution, with values of 2.583, 2.787, and 5.383 Å, respectively. The η^2 coordination of the olefinic double bond is maintained throughout this step, with Pd−C bond distances of 2.450, 2.493 Å in **TSDTC1** and 2.412, 2.449 Å in **IDTC2**. In the resulting intermediate **IDTC2** the η^2 C−C bond of the organoboronate ligand has changed orientation and is perpendicular with respect

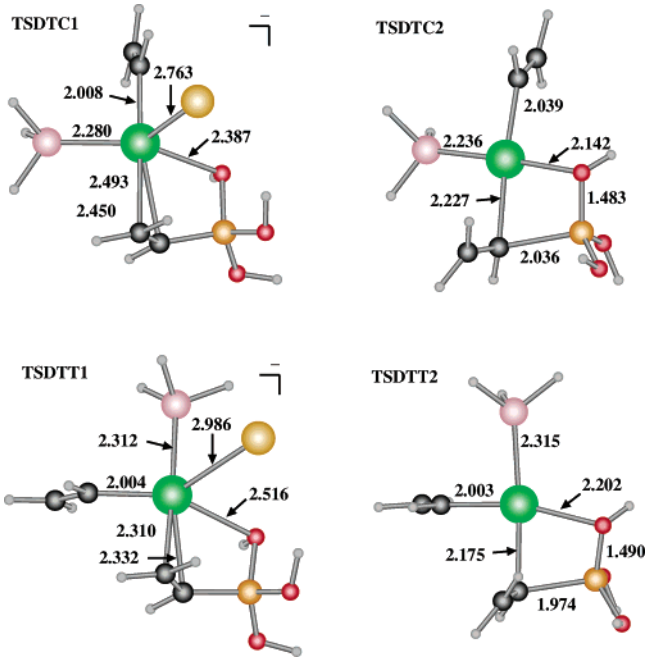

Figure 14. Becke3LYP-optimized geometries of the transition states corresponding to the transmetalation step of the dissociative mechanism.

to the plane of the complex. Rotation of this type of double bonds in the metal coordination sphere often presents low barriers.[47] The second step in this DTC mechanism is the obtention of intermediate **IDTC3** through transition state **TSDTC2** (Figure 14). In this step, the B−C bond is cleaved, and the vinyl coordination shifts from η^2 to η^1. The reaction can be again well followed by the variation in the distances in the stationary points. The Pd−C bond being strengthened goes from 2.412 Å in **IDTC2** to 2.227 Å in **TSDTC2** to 2.105 Å in **IDTC3**. The B−C bond varies in the opposite sense: 1.646 Å in **IDTC2**, 2.036 Å in **TSDTC2**, and 3.587 Å in **IDTC3**.

The energetics in the DTC path are quite smooth from **IDTC1** to **IDTC3**. The reaction is exothermic by 9.6 kcal/mol, and the highest energy point, **TSDTC2**, is only 12.6 kcal/mol above the lowest energy intermediate **IDTC1**. Formation of **IDTC1** from **10** and **16** is however quite exothermic (30.5 kcal/mol),

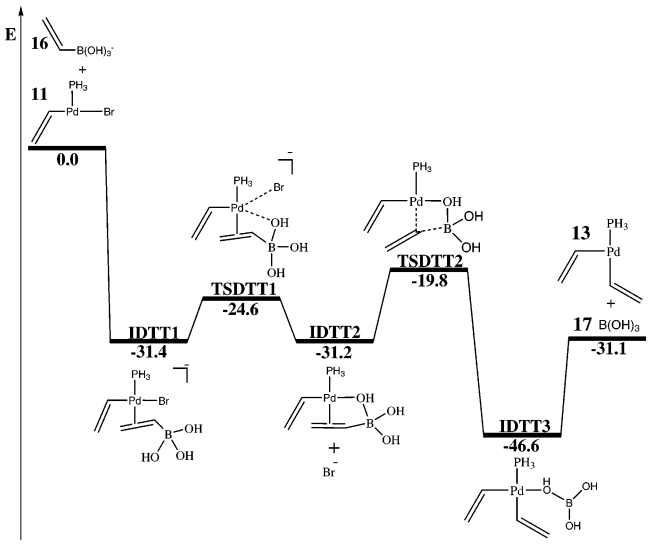

Figure 15. Energy profile for the *trans* alternative of the transmetalation step in the dissociative mechanism.

and release of $B(OH)_3$ from **IDTC3** to generate the three-coordinate product **12** is quite endothermic (23.0 kcal/mol). These large energy differences suggest that the three-coordinate species **10** and **12** may not exist as such and that the departure of the fourth ligand is coupled to the entry of a replacing group, with the possibility of this being a solvent molecule.[15]

The last of the possible transmetalation processes is the *trans* dissociative pathway, labeled as DTT, which starts from the three-coordinate complex **11**, where vinyl and bromide are *trans* to each other. The corresponding energy profile is shown in Figure 15 and is qualitatively similar to that of the DTC path. There are also three intermediates and two transition states. The first intermediate, **IDTT1**, is obtained when the double bond of the vinyl group coordinates to Pd, with Pd−C bond distances of 2.403 and 2.287 Å, and it has an energy 31.4 kcal/mol below the separated **11** and **16** molecules. The first transition state, **TSDTT1**, shown in Figure 14, corresponds to the displacement of bromide by one of the hydroxyl groups of the boronate (Pd−Br, 2.986 Å; Pd−O, 2.516 Å). The second transition state, **TSDTT2**, also in Figure 14, corresponds to the cleavage of the B−C bond and the shift of the vinyl from η^2 to η^1 (B−C, 1.974 Å; Pd−C 2.175 Å). The minor discrepancies between the geometries of the *cis* and *trans* paths for this dissociative transmetalation step can be easily explained by the different *trans* influence of the phosphine and vinyl ligands.

The energy pattern for the DTT path is also similar to that of the DTC mechanism. The reaction is very smooth from **IDTT1** to **IDTT3**, with an exothermicity of 15.2 kcal/mol and a highest energy point (**TSDTT2**) 11.6 kcal/mol above **IDTT1**. The initial approach of boronate **16** to the three-coordinate species **11** is very exothermic (31.4 kcal/mol), and the final release of $B(OH)_3$ to yield the three-coordinate divinyl species **13** is quite endothermic (15.5 kcal/mol). This further suggests the presence of additional ligands able to stabilize to some extent these three-coordinate intermediates.

5.4. Second Isomerization. If the transmetalation takes place through the *cis* dissociative path, the resulting complex **12** has the two vinyl ligands in a *trans* arrangement. The subsequent reductive elimination is not possible from this isomer, and an isomerization step is necessary to convert it into complex **13**, where the two vinyl groups are *cis*. This isomerization occurs through transition state **TSDS**, which has been discussed above as **TSAST** within this same step of the associative mechanism. The energy barrier for the process is quite low; **TSDS** is 9.6 kcal/mol above **12**.

The transmetalation step starting from the *trans* complex, **11**, ends up in complex **13**, where both vinyl groups are in *cis* position. The subsequent reductive elimination can take place directly from this species, and no further isomerization is needed.

5.5. Reductive Elimination. In the reductive elimination step, the R−R′ molecule is released from the LPd(R)(R′) complex. In our model system, this reductive elimination takes place directly from the three-coordinate complex **13**, where the two vinyl groups are *cis*. Transition state **TSDE** is reached quite early in the reaction path, the C−C distance of the bond being formed is quite long (2.238 Å), and the Pd−C bonds are minimally elongated with respect to the values in **13** (from 1.999 to 2.019 Å, and from 1.998 to 2.031 Å, respectively). This is however consistent with the very low barrier for the reaction (1.4 kcal/mol) and with the large exothermicity. Intermediate **IDE**, where the divinyl product is coordinating η^2 to the monophosphine complex, is 49.2 kcal/mol more stable than **13**. Separation of the product from palladium to regenerate the catalyst has an energy cost of 23.7 kcal/mol, again suggesting the possible participation of an external group to favor this step.

Discussion

Figures 16 and 17 summarize the results presented above for the associative and dissociative mechanisms, respectively. For each step (oxidative addition, isomerization, transmetalation, reductive elimination) the computed energy barrier has been included. In the case of multistep processes, which are simplified in these figures for clarity, the barrier is calculated as the energy difference between the lowest energy intermediate and the highest energy transition state. The energy cost of elementary steps involving ligand dissociation (phosphine, boric acid, divinyl product, etc.) from palladium has also been neglected.

A first important result from Figures 16 and 17 is that all energy barriers involved are lower than 25 kcal/mol, a result that would remain likely unchanged if ligand dissociation energies were accurately introduced. All the processes presented would thus be feasible at room temperature, or with a minimum heating. Therefore, the mechanistic problem is not the discovery of a reasonable mechanism within a group of mostly forbidden alternatives, but to choose the preferred one between a manifold of energetically reasonable mechanisms.

The formally most simple pathway is that going through the *cis* transmetalation in the associative mechanism (Figure 16). This is the only case where neither phosphine loss nor isomerization is necessary, and the highest barrier is relatively low, 20.8 kcal/mol.

It is worth noticing that the *trans* transmetalation (path ATT) in the same associative mechanism has a higher barrier than the *cis* transmetalation. This result is not necessarily extrapolable to all experimental systems because of the lack of steric bulk in our model phosphines. This result nevertheless suggests that the usual assumption in the textbook mechanism of a mechanism going through the *trans* four-coordinate diphosphine may be incorrect in at least some cases. It could well be that the *trans* diphosphine is observed, but that the reaction goes through the *cis* isomer. The isomerization steps that are necessary for access to the associative *trans* path have small barriers, although they are complicated by the fact that they require a (at least temporary) change in the number of phosphine ligands attached to the metal.

Interpretation of the scheme for the dissociative mechanism associated with the monophosphine systems, presented in Figure

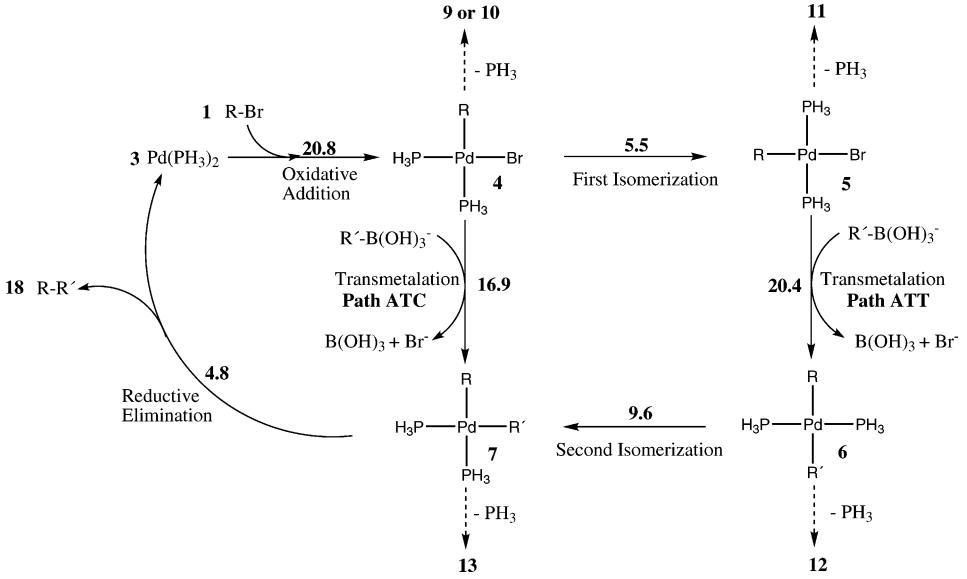

Figure 16. Final proposal for the associative reaction mechanism, with two phosphine ligands. The highest energy barrier involved in each reaction step is indicated in kcal/mol.

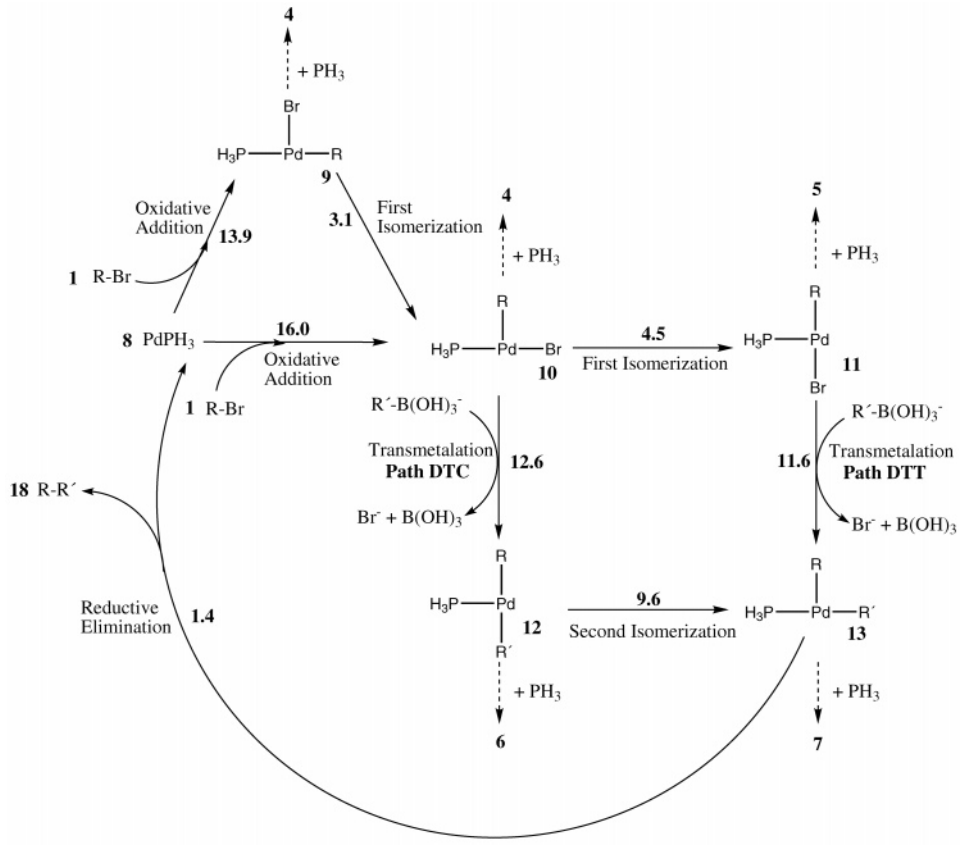

Figure 17. Final proposal for the dissociative reaction mechanism, with one phosphine ligand. The highest energy barrier involved in each reaction step is indicated in kcal/mol.

17, is somehow more complicated. As mentioned above, the cost corresponding to ligand release is omitted from the scheme, and there are several of these steps. A phosphine has first to dissociate from the initial diphosphine complex to obtain the monophosphine catalyst. The release of $B(OH)_3$ from the transmetalation products has a relatively high cost in terms of potential energy (up to 23.0 kcal/mol for the *trans* path), and this is also the case for release of the divinyl product after the reductive elimination step (23.7 kcal/mol). These barriers to dissociation arise from the difficulty of eliminating ligands from quite unsaturated complexes and would be surely significantly diminished by the explicit introduction of other coordinating groups, like solvent molecules, free phosphine, or additional molecules of substrate or product. If we do not take into account these dissociation steps, the resulting energetics in Figure 17 indicate a set of dissociative pathways that are very competitive with the associative mechanisms presented above. The lowest energy path would go succesively through all three LPd(R)(Br) isomers (via two isomerizations) and the *trans* mechanism for transmetalation. The highest energy barrier

would be in the oxidative addition step, with a value of 13.9 kcal/mol.

The main result to be extracted from Figures 16 and 17 is that most of the mechanistic possibilities considered are feasible. In this way, the reported observation by Goossen, Thiel, and co-workers is confirmed in a more general model.[21] The four different transmetalation channels have reasonable barriers, and they can be accessed by isomerization steps requiring moderate energies. The identity of the most favored mechanism will likely depend on the specific nature of phosphine, substrate, and solvent for each case and cannot be answered by a study on a general model like this one. On the contrary, this general study is conclusive in indicating that a variety of mechanistic possibilities has to be considered and that they cannot be discarded a priori.

Our results also indicate that the associative and dissociative catalytic cycles are not mutually exclusive. The first isomerization step in the associative mechanism may require phosphine dissociation, and the second one almost surely does. The ligand release steps in the dissociative mechanism are likely facilitated by the association of additional ligands. There are a number of points where both ideal mechanisms can intercross, either by addition or subtraction of a phosphine ligand, and they are marked in the figures by dashed arrows. It is therefore logical to expect that in the real systems the mechanism is often going to be a mixture of both possibilities. It is possible to envision situations where oxidative addition takes place in a dissociative scheme and reductive elimination in an associative one. It is also possible to have some of the steps, for instance oxidative addition, coupled to phosphine elimination. These results also lend support to the possibility of the eventual participation of additional species in solution as ligands, in what has been labeled as anionic mechanisms.[15,21]

7. Conclusion

The mechanism for the full catalytic cycle of the Suzuki−Miyaura cross-coupling between CH_2═CHBr and CH_2═CHB-$(OH)_2$ has been analyzed by means of Becke3LYP DFT calculations. A manifold of paths has been characterized with low energy barriers acceptable for a process taking place at room temperature. In particular, the transmetalation step can proceed smoothly with either one (dissociative mechanism) or two (associative mechanism) phosphine ligands at palladium and can occur with either *cis* or *trans* arrangements of the ligands around the metal. The use of a general model, with PH_3 as phosphines and vinyls as coupling groups, does not allow this set of calculations to predict what would be the definitive path for a given experimental system. In fact, these results strongly suggest that different detailed mechanisms will occur in different experimental systems. Specific studies with explicit consideration of the particular substrates, phosphine substituents, and solvent will be necessary for the elucidation of the detailed mechanism operating on a given experimental system. We are currently working on this type of studies in our laboratory.

Acknowledgment. Financial support from the ICIQ foundation, from the Spanish MEC through Projects CTQ2005-09000-CO1-01 (G.U.) and CTQ2005-09000-CO1-02 (A.A.C.B., F.M.), and from the Catalan DURSI through projects 2005SGR00715 (A.A.C.B., F.M.) and 2005SGR00896 (G.U.) is acknowledged. G.U. thanks the Spanish MEC for a "Ramón y Cajal" contract.

Supporting Information Available: PDF file containing the full ref 36 and Cartesian coordinates and total energy for all computed structures. This material is available free of charge via the Internet at http://pubs.acs.org.

OM060380I